



ELSEVIER

Contents lists available at ScienceDirect

Nuclear Instruments and Methods in Physics Research A

journal homepage: www.elsevier.com/locate/nima

Tomographic characterisation of gas-jet targets for laser wakefield acceleration

J.P. Couperus^{a,b,*}, A. Köhler^{a,b}, T.A.W. Wolterink^c, A. Jochmann^a, O. Zarini^{a,b},
H.M.J. Bastiaens^c, K.J. Boller^c, A. Irman^a, U. Schramm^{a,b}

^a Helmholtz-Zentrum Dresden – Rossendorf, Institute of Radiation Physics, Bautzner Landstrasse 400, 01328 Dresden, Germany

^b Technische Universität Dresden, 01069 Dresden, Germany

^c University of Twente, PO Box 217, 7500 AE Enschede, The Netherlands

ARTICLE INFO

Article history:

Received 8 October 2015

Received in revised form

21 January 2016

Accepted 29 February 2016

Keywords:

Laser wakefield acceleration

LWFA

Gas-jet analysis

Interferometry

Tomography

ABSTRACT

Laser wakefield acceleration (LWFA) has emerged as a promising concept for the next generation of high energy electron accelerators. The acceleration medium is provided by a target that creates a local well-defined gas-density profile inside a vacuum vessel. Target development and analysis of the resulting gas-density profiles is an important aspect in the further development of LWFA.

Gas-jet targets are widely used in regimes where relatively high electron densities over short interaction lengths are required (up to several millimetres interaction length, plasma densities down to $\sim 10^{18} \text{ cm}^{-3}$). In this paper we report a precise characterisation of such gas-jet targets by a laser interferometry technique. We show that phase shifts down to 4 mrad can be resolved. Tomographic phase reconstruction enables detection of non-axisymmetrical gas-density profiles which indicates defects in cylindrical nozzles, analysis of slit-nozzles and nozzles with an induced shock-wave density step. In a direct comparison between argon and helium jets we show that it cannot automatically be assumed, as is often done, that a nozzle measured with argon will provide the same gas density with helium.

© 2016 Elsevier B.V. All rights reserved.

1. Introduction

Laser wakefield acceleration (LWFA) [1] is a promising concept for the next generation of compact electron accelerators. Using the wakefield created by an ultra-short laser pulse travelling through an underdense plasma, acceleration gradients can be as high as 100 GV/m, three to four orders of magnitudes higher than in conventional RF accelerators. Ever since the first demonstration of LWFA in 1994 [2] the field is quickly developing. Recently generation of Multi GeV electron beams with energies up to 4.2 GeV, 6% rms energy spread and 9 pC charge have been reported by channelling a 0.3 PW ultra-short pulse in a 9 cm long capillary discharge waveguide [3]. However, many challenges in laser wakefield accelerators still remain. Main challenges are on how to improve shot-to-shot energy and pointing stability, energy spread and achievable charge per bunch. For further optimisation of the LWFA process it is crucial to have exact knowledge of the medium in which the acceleration takes place. Besides capillaries, gas-jet targets are the main provider for acceleration media in

LWFA. In this paper we present characterisation of such LWFA gas-jet targets by laser-interferometry. For axisymmetrical targets we perform a reconstruction method based on an Abel-inversion algorithm which gives the gas-density distribution. Using helium as a fully ionisable gas, this provides the electron density distribution n_e for LWFA. However, due to the low refractive index of helium gas, interferometric phase shift measurements are challenging. One can rely on the use of higher refractive gases like argon or nitrogen [4–6], but as we show in Section 3.2 this does not necessarily represent the exact gas density profile of the same nozzle operated with helium gas. Therefore we use an ultra sensitive interferometric setup in order to perform measurements on helium directly.

Targets providing longer interaction lengths or gas-density steps normally do not possess axisymmetry. For these kind of targets we use a tomographic reconstruction algorithm.

2. Method of analysis

2.1. Experimental setup

In interferometry, the presence of the gas induces an optical path length difference between the probe arm and a reference arm

* Corresponding author at: Helmholtz-Zentrum Dresden – Rossendorf, Institute of Radiation Physics, Bautzner Landstrasse 400, 01328 Dresden, Germany.

E-mail address: j.couperus@hzdr.de (J.P. Couperus).

resulting in a phase shift on the interferogram. A schematic of our setup is shown in Fig. 1. The Mach-Zehnder type interferometer consists of a 18 mW continuous wave HeNe laser at 632.8 nm (Linios G040-814-00 with PS-3170). Depending on the nozzle size, the laser beam is expanded to illuminate the entire gas-jet by lenses L1 and L2 in a telescope configuration. In this telescope we spatially filter the beam using a pinhole to acquire a spatially homogeneous beam. Both interferometer arms have approximately the same length to stay within the coherence length of the laser. 50:50 beamsplitters (BS1 & BS2) are used to achieve the highest interferometric fringe contrast. The arms overlap at a CCD camera (PCO.pixelfly) which is positioned at the image plane of the gas-jet created by lens L3. Temporal resolution is achieved by short (μs range) camera exposure. A small angle α introduced at BS2 results in a fixed sinusoidal interference pattern along the x -direction according to [7,8]

$$I = 2I_0 [1 + \cos(kx \sin(\alpha))] \quad (1)$$

where $k = (2\pi)/\lambda_L$ is the laser wavenumber. This constant pattern acts as the carrier pattern, which is necessary as a carrier for the phase-shift that the gas-jet induces in the signal arm.

The gas-jet in the signal arm introduces an optical path length difference (ΔOPL), which adds to the intensity function which is imaged on the CCD:

$$I = 2I_0 \left(1 + \cos \left(kx \sin(\alpha) + \frac{2\pi \Delta OPL}{\lambda_L} \right) \right) \quad (2)$$

with $\Delta OPL = \int_C \Delta n(s) ds$.

The term within the cosine contains both the above-mentioned carrier contribution as well as the contribution from the gas-jet induced phase shift. The optical path length difference depends on the density distribution of the gas-jet and its associated refractive index change $\Delta n(s)$ along a path C .

2.1.1. Setup stability

Besides the phase shift introduced by the gas-jet, disturbances like air flow, irregularities in optics and scattered laser-light add unwanted extra phase disturbances. Including these extra influences and rewriting Eq. (2) gives

$$I(x, y) = I_A(x, y) + I_B(x, y) \cos [\varphi_c(x, y) + \varphi_s(x, y) + \varphi_d(x, y)]. \quad (3)$$

The CCD-chip defines the x, y -plane. I_A is the background and I_B the local amplitude of the fringe function, which may vary in the

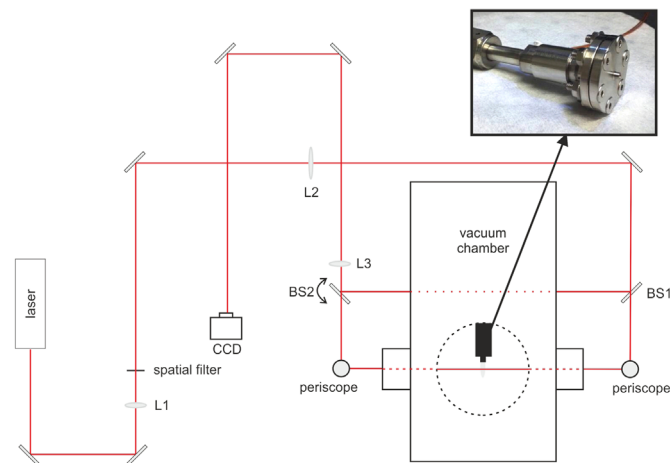


Fig. 1. Schematic representation of the gas-jet interferometry setup. Lenses L1 & L2 function as a beam expander. L3 images the target plane onto the CCD. The inset shows a 0.75 mm cylindrical nozzle. For tomography purposes the gas-jet target can be rotated to take measurements under multiple angles.

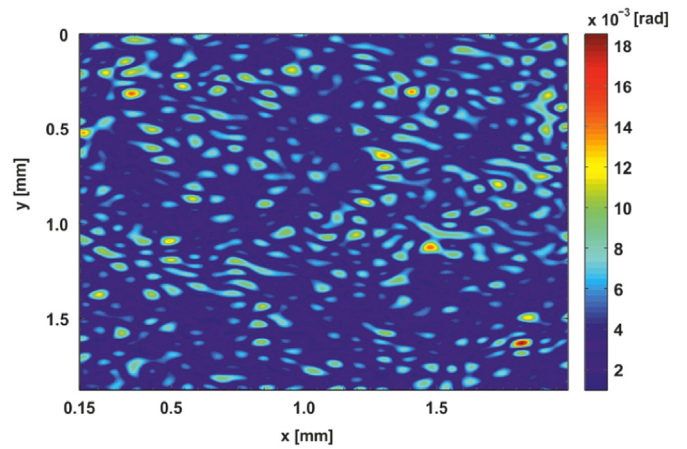


Fig. 2. Standard deviation map over 30 measurements. The phase map was constructed when no jet was present and shows the stability of the setup.

case of a non-uniform illumination. φ_c is the carrier phase and φ_s is the signal phase, they correspond to the first and second part within the cosine of Eq. (2) respectively. φ_d contains all disturbances that do not come from the static fringe pattern or the gas jet. The setup has been optimised to keep φ_d as low as possible. This is achieved by using active vibration isolation of the optical table, encasement to minimize air-turbulences and dust scattering and placing optics away from the imaging plane so unwanted scattering from optics defects do not image to the camera plane.

Fig. 2 shows a noise map of the setup. This map is constructed by taking measurements under experimental conditions but without a gas-jet present. Ideally, every single measurement should render the exact same phase map. Small fluctuations in setup stability introduce phase disturbances φ_d for every shot. The shot-to-shot standard deviation is a measure for the noise in the setup. Overall, the average standard deviation is 3.9×10^{-3} rad, well below the shift expected for the gas-jet targets.

2.2. Data processing

After acquisition of the images, we further process the data to reconstruct the gas density profile. This is done in two steps: phase retrieval (Section 2.2.1), followed by gas density reconstruction, by Abel-inversion or tomographic reconstruction (Section 2.2.2).

2.2.1. Phase retrieval

A typical interferogram can be seen in Fig. 3(a). This image contains all the information as expressed in Eq. (3). Since only the phase shift φ_s is of interest, data-processing is required to extract this information. Using the Fourier-transform method [9] we transform the image into the Fourier domain to filter the phase information. Rewriting Eq. (3) in the frequency domain gives:

$$\hat{I}(f_x, f_y) = \hat{I}_A(f_x, f_y) + \hat{I}_C(f_x - f_{c,x}, f_y - f_{c,y}) + \hat{I}_C^*(f_x + f_{c,x}, f_y + f_{c,y}) \quad (4)$$

where the hat denotes the Fourier transform and the asterisk superscript denotes the complex conjugate. At this stage a frequency filter is applied to the Fourier transform. Only the $\hat{I}_C(f_x - f_{c,x}, f_y - f_{c,y})$ part is selected. A two-dimensional representation of this process is shown in Fig. 4. By defining the range of the filter, noise components outside this range are filtered out.

Performing a back Fourier transformation over the selected filter gives an intensity according to Eq. (3). The background variation is contained in the real part and the phase in the imaginary

Download English Version:

<https://daneshyari.com/en/article/8168542>

Download Persian Version:

<https://daneshyari.com/article/8168542>

[Daneshyari.com](https://daneshyari.com)